Competing ordered structures formed by particles with a regular tetrahedral patch decoration

Günther Doppelbauer[1,⋆], Eva G. Noya[2,⋆], Emanuela Bianchi[1], and Gerhard Kahl[1]

[1]Institut für Theoretische Physik and Center for Computational Materials Science (CMS), Technische Universität Wien, Wiedner Hauptstraße 8-10, A-1040 Wien, Austria

[2]Instituto de Química Física Rocasolano, CSIC, Calle Serrano 119, E-28006 Madrid, Spain

⋆ authors who contributed equally to this work

E-mail: guenther.doppelbauer@tuwien.ac.at

Date: 28 February 2012

Abstract. We study the ordered equilibrium structures of patchy particles where the patches are located on the surface of the colloid such that they form a regular tetrahedron. Using optimization techniques based on ideas of evolutionary algorithms we identify possible candidate structures. We retain not only the energetically most favourable lattices but also include a few energetically less favourable particle arrangements (i.e., local minima on the enthalpy landscape). Using suitably developed Monte Carlo based simulations techniques in an NPT ensemble we evaluate the thermodynamic properties of these candidate structures along selected isobars and isotherms and identify thereby the respective ranges of stability. We demonstrate on a *quantitative* level that the equilibrium structures at a given state point result from a delicate compromise between entropy, energy (i.e., the lattice sum) and packing.

Submitted to: *J. Phys.: Condens. Matter*

1. Introduction

Patchy particles are colloidal entities whose surfaces are decorated by well-defined regions, which differ in their interaction behaviour significantly from the one of the "naked" colloidal surface (for an experimental and theoretical overview see [1] and [2], respectively). Since these regions can be positioned with high accuracy on the particle surface and the spatial extent of the patches can be tuned in suitable chemical or physical synthesis processes, the highly directional and selective interactions of patchy particles have promoted them as very promising entities that are able to self-assemble into larger target units with desired physical properties.

The central problem that has to be overcome to achieve this goal is to acquire a profound understanding of the self-assembly strategies of patchy particles characterized by a particular patch decoration. During past years, considerable effort has been dedicated to solve this intricate and challenging problem via different numerical and methodological routes [3, 4, 5, 6, 7]. In another contribution [8] we have demonstrated that a suitable combination of two complementary numerical approaches is able to provide a highly satisfactory answer to this yet open issue. To be more specific, we have combined the following two methods: (i) on one hand, an optimization technique, which employs ideas of evolutionary algorithms [9] that is able to predict efficiently and with high reliability ordered equilibrium structures at *vanishing* temperature; (ii) on the other hand, suitably developed Monte Carlo simulations [10, 11] which allow to evaluate accurately, via thermodynamic integration, the thermodynamic properties of a particular ordered structure formed by patchy particles at *finite* temperature. The most favourable structures with respect to the enthalpy identified in the first step are considered in the second step as candidate configurations at finite temperature. The combination of the two complementary approaches compensates thus for the respective limitations of the two methods: (i) the risk to lose candidate structures in a preselection process is now suppressed due to the systematic search of candidate structures performed in the optimization step; and (ii) the evaluation of the thermodynamic properties of the systems at finite temperature is now guaranteed by highly reliable and accurate simulations.

In this contribution we focus on a system of patchy particles where the patches are positioned in such a way that they form a regular tetrahedron on the colloidal surface. The ordered equilibrium structures at zero temperature and the (pressure vs. temperature) phase diagram obtained via the combined approach outlined above have been shown and discussed in [8]. Several aspects that could not be presented in this rather concise presentation are discussed in detail in the present contribution. In particular, we will focus in the following not only on the energetically most favourable structures as they are suggested at vanishing temperature by the optimization approach (corresponding to *global* minima in enthalpy at a given pressure value), but also consider those lattices that represent *local* minima, which differ from the optimal solution by a few percent. For all these structures we have evaluated in a subsequent step their

thermodynamic properties via our simulation based thermodynamic integration scheme along selected isobars and isotherms. From this detailed analysis we can obtain a deeper insight into the complex competition between entropy, energy (i.e., the lattice sum), and packing which finally defines for a given state point the energetically most favourable ordered structure.

The paper is organized as follows: in the subsequent section we briefly present the patchy particle model and give a short summary of the methods used in this contribution. Results are summarized and discussed in section 3 and the paper is closed with concluding remarks.

2. Model and theoretical tools

2.1. The model

We use a standard model for patchy particles, that has been proposed by Doye *et al.* [13] and has been employed in a number of contributions by different researchers (e.g., see [14, 5, 15, 16, 9, 17]). The interaction between two patchy particles is based on a spherical Lennard-Jones potential with the usual parameters ϵ and σ, which specify energy and length units; for interparticle distances $r > \sigma$, this interaction is multiplied by a factor $0 \leq V_{\text{ang}} \leq 1$, which depends on the relative orientations of the particles. Thus, the repulsive part of the Lennard-Jones potential models the spherical colloids, while its attractive part multiplied by V_{ang} models the attraction between the patches.

The spatial extent of the patches is characterized by a parameter, for which we have chosen the same value as in [5, 8].

2.2. Theoretical tools

To identify possible candidate structures for the phase diagram at *vanishing* temperature we have used optimization strategies based on ideas of evolutionary algorithms. Such algorithms incorporate concepts of Darwinian evolution in order to tackle optimization problems, i.e., finding extremal values of a cost function $f = f(\mathbf{x})$, where $\mathbf{x}$ is a vector in the parameter search space. A pool of candidate solutions is treated as a "population", which undergoes an evolutionary process, including the following operations: selection (i.e., candidate solutions with lower cost function values are more likely to survive within the population and reproduce), reproduction (i.e., features of existing candidate solutions are recombined in order to produce new candidates) and mutation (i.e., features of candidate solutions are randomly modified). We are using a so-called phenotype implementation of an evolutionary algorithm, which combines the aforementioned global optimization steps with local ones, using a limited memory algorithm for bound constrained optimization, relying on the computation of first derivatives of the cost function $\partial f/\partial \mathbf{x}$ [18]. For details we refer to [19, 9, 20, 21].

Our investigations have been carried out in an isobaric-isothermal ensemble. Thus, the cost function is the Gibbs free energy G, which, at vanishing temperature,

reduces to the enthalpy H, given by $H = U + PV$, U being the lattice sum, P the pressure, and V the volume of the system. The vectors $\mathbf{x}$ in search space collect the lattice parameters and the coordinates of the particles within the primitive cell. The particle number being N, we define dimensionless quantities by introducing the packing fraction $\eta = (\pi/6)(N\sigma^3/V)$, the reduced enthalpy $H^\star = H/(N\epsilon)$, the reduced energy $U^\star = U/(N\epsilon)$ and the reduced pressure $P^\star = P\sigma^3/\epsilon$; thus, $H^\star = U^\star + (\pi/6)(P^\star/\eta)$. At some fixed pressure value, we record during the evolutionary process not only the lattice corresponding to the global enthalpy minimum, but also ordered structures that represent low-lying local minima on the enthalpy landscape (differing typically by less than twenty percent from the energetically most favourable lattice).

For these candidate structures the thermodynamic properties at *finite* temperature (measured in the dimensionless quantity $T^\star = k_\mathrm{B}T/\epsilon$) have then been calculated in simulations via thermodynamic integration. For this task we have used a suitably adapted Monte Carlo code, described in detail in [11, 5]. Briefly, we calculated the Helmholtz free energy (A) for each solid phase at a given thermodynamic state using the Einstein molecule method [5]. In this method the free energy is calculated by thermodynamic integration using as a reference an Einstein crystal with the same structure as the solid of interest, in which the orientation of the particles is imposed by an orientational field. For this crystal, the free energy can be numerically evaluated [5]. Once the Helmholtz free energy of a given phase is known at one thermodynamic state, its value can be calculated at any other thermodynamic state by thermodynamic integration. The stability of the structures at finite $T^\star$ is governed by the minimization of the chemical potential which is given by:

$$\mu/k_BT = G/Nk_BT = A/Nk_BT + PV/Nk_BT,$$

or, in reduced units,

$$\mu^\star/T^\star = A^\star/T^\star + P^\star V^\star/T^\star,$$

where $\mu^\star = \mu/\epsilon$, $A^\star = A/(N\epsilon)$ and $V^\star = V/(N\sigma^3)$). When comparing the thermodynamic properties of two competing structures, the relevant quantity is the difference in the chemical potential, $\Delta\mu^\star$. Thus, the dependence of the absolute $\mu^\star$ values on the chosen reference structure does not influence the phase diagram, as long as the same reference is used for all phases.

3. Results

3.1. Structural variations along isobars

Figures 1 and 2 visualize the ordered structures that correspond to the lowest-lying local enthalpy minima for $P^\star = 2.5$ and $P^\star = 4.5$, respectively (these values where chosen as particularly interesting based on the knowledge of the $(P^\star, T^\star)$-phase diagram [8]). The top panel shows, along with the respective enthalpy values, the two relevant contributions to this quantity, namely the lattice sum and the packing fractions as

bars. These quantities are shown in relative units of the corresponding values of the energetically most favourable lattice structures: thus, $U_{\rm i}/U_{\rm opt} > 1$ (< 1) - where the index "i" stands for any of the considered structures and the index "opt" indicates the most favourable lattice (i.e., structure "a" for $P^\star = 2.5$ and "f" for $P^\star = 4.5$) - correspond to a higher (lower) degree of bond saturation than realized in the optimal particle configuration. Similarly, $\eta_{\rm i}/\eta_{\rm opt} > 1$ (< 1) indicates a better (worse) packing of particles as compared to the energetically most favourable lattice. In Figures 3 and 4 the internal energies and the packing fractions of the structures investigated are displayed as functions of temperature along the two isobars as obtained by Monte Carlo simulations.

Before we start the discussion of structural variations along two selected isobars, we mention two structures, that have raised quite some interest in the literature [12, 7, 5], namely diamond cubic and diamond hexagonal phases (especially the former, which has potential use in the fabrication of materials with photonic band gaps [22]). In our calculations, these structures appear as corresponding to low-lying minima on the enthalpy landscape for very low pressure values, but as discussed in [5], are never stable for the values of the potential parameters we are using in this contribution.

3.1.1. Isobar at $P^\star = 2.5$ The six most favourable structures with respect to the enthalpy, identified at $P^\star = 2.5$ are summarized in Figure 1 (labeled in this Figure and in the following by "a" to "f") along with an analysis of how the respective values for the enthalpy are split up into the lattice sum and the packing fraction.

The global enthalpy minimum for this pressure value corresponds to, as previously reported in [12, 5, 8], a bcc-like structure that consists of two interpenetrating, but virtually non-interacting diamond lattices. This structure emerges in two different, but closely related versions: the particles of one diamond sublattice can be located exactly in the centers of the voids of the six-particle rings making up the other diamond sublattice ("b" in Figure 1) or the positions of the particles in each sublattice can be slightly shifted against each other ("a" in Figure 1). At $T^\star = 0$, the latter structure is energetically more favourable: its enthalpy value is by 0.3 percent smaller as compared to the enthalpy of the former. This can be understood by the fact that the bond lengths of the shifted configuration are slightly closer to the ideal value (i.e., the position of the minimum of the Lennard-Jones potential) at the same packing fraction ($\eta = 0.54$) as the symmetric configuration. Already at a minute value of temperature, these two structures become indistinguishable (cf. Figure 3).

Configuration "c", which has the third-lowest enthalpy value at $P^\star = 2.5$ and vanishing temperature, is also closely related to the double diamond configuration: compared to structure "b", bonds between two oppositely located pairs of particles within each six-particle ring are broken (see pale green patches displayed in panel "c" of Figure 1); the emerging half-rings are slightly distorted and displaced with respect to each other. This results in a higher packing fraction (by 9.8 %) but a substantial increase in the lattice sum (by 14.2 %); in total this leads to an increase in the enthalpy by 10.5 % with respect to the energetically most favourable particle arrangement at $P^\star = 2.5$

("a"). We note that at vanishing temperature structure "c" becomes more favourable than the fully bonded ones at $P^\star = 3.2$ (see Figure 6, top panel). However, at finite temperature, as entropic effects set in, the relatively low enthalpy value is soon overruled: our simulation results indicate that the structure is only stable for temperatures up to $T^\star \simeq 0.006$.

For structure "d", corresponding to the fourth-lowest local enthalpy minimum, the discrepancy between bonding and packing is even more pronounced: we identify a relatively dense configuration ($\eta = 0.63$), consisting of hexagonally arranged particles, where each layer is strongly bonded with one of its neighbouring layers and unconnected with the other one. To be more specific, each particle forms bonds via three of its patches: two of these bond with particles within the same layer, the third one connects the particle to a neighbouring layer. Our simulations at finite temperature show that this configuration is never the most stable one in the $(P^\star, T^\star)$-phase diagram.

The structure representing enthalpy minimum five is a non-close packed ($\eta = 0.68$) fcc-like lattice ("e" in Figure 1), where each particle has two saturated bonds. Within the fcc-picture, the particles located at the vertices of the cube differ in their orientation from the particles that occupy the centers of the faces. Despite its high packing fraction, this structure is never stable at vanishing temperature due to the small number of saturated bonds. However, a slightly modified version of this lattice (previously discussed in [5]), where each particle is rotated in order to replace a single, fully saturated bond by two weaker bonds, is found to be stable at finite temperatures in the $(P^\star, T^\star)$-phase diagram [8] for $T^\star \gtrsim 0.06$ over a pressure range steadily increasing with temperature.

Structure "f", corresponding to the sixth local enthalpy minimum, is another fcc-like configuration, which achieves a relatively high value for the packing fraction, namely $\eta = 0.71$ (compared to $\eta = 0.74$ for close packed hard spheres). Again, each particle forms two bonds and particles located at different positions in the cubic cell are oriented in two different directions. For pressure values above $P^\star = 3.4$, this structure corresponds to the global enthalpy minimum at $T^\star = 0$ and has a broad region of stability at finite temperature [8].

In Figure 3 we have depicted our MC results for the internal energy $U^\star$ and for the packing fraction η evaluated for the six lattice structures considered at $P^\star = 2.5$ over a representative temperature range. The curves are shown over the respective ranges of mechanical stability for each ordered structure. Note that the simulation data for $U^\star$ and η can smoothly be extrapolated for $T \to 0$ to the respective values obtained via the optimization algorithm which nicely demonstrated the internal consistency of our combined approach. The $U^\star$- and η-curves for lattices labeled "a" and "b" become essentially indistinguishably close, even for the smallest finite temperature investigated. In the displayed temperature range no phase transition takes place (cf. [8]).

As expected we observe a monotonous increase of $U^\star$ with temperature for all structures ("a" to "f"), giving evidence that the bond saturation decreases with increasing $T^\star$. From the smoothness of the curve one can conclude that no structural transition takes place in the displayed temperature interval. Concomitantly the packing

fraction decreases – as expected – monotonically with increasing temperature. It should be emphasized that for the energetically most favourable structure(s) ("a" and "b") the packing fraction remains essentially constant within the observed temperature interval.

3.1.2. Isobar at $P^\star = 4.5$ For this pressure value, we have considered the structures that correspond to the four lowest lying local enthalpy minima; among those lattices two ("e" and "f" in Figure 1) have already been discussed for the case $P^\star = 2.5$. The other two structures, labeled "g" and "h" are depicted in Figure 2.

The global minimum in enthalpy at vanishing temperature still corresponds to the almost close-packed fcc-like structure described above ("f" in Figure 1). The second-lowest minimum of the enthalpy landscape corresponds to an hcp-like structure ("g" in Figure 2). Similar to the packed fcc-like case, each particle forms two bonds – one with a particle within the same layer, the other connecting to a particle in a neighbouring layer; however, here the bonding angles are found to be considerably closer to the ideal values (i.e., the patches directly face each other), resulting in a slightly lower lattice sum $U^\star$. Nevertheless, the packing fraction of this structure ($\eta = 0.70$) is again lower, rendering it, in total, less favourable than configuration "f". The third local enthalpy minimum is represented by another hcp-like structure ("h" in Figure 2). Similar to the hexagonal configuration mentioned in the previous paragraph ("d" in Figure 1), each particle forms two intra-layer bonds; however, in configuration "h", there are no inter-layer bonds at all. This lattice reaches a packing fraction similar to the one of the global minimum structure ("f") (at vanishing and very low $T^\star$ it is even slightly higher); however, it has a considerably higher $U^\star$-value, making it thus unstable in the entire $(P^\star, T^\star)$-phase diagram. Local minimum four corresponds to the non-close-packed fcc-like structure already identified at $P^\star = 2.5$ ("e" in Figure 1).

In Figure 4 we display $U^\star$ and η as functions of temperature which show – as expected – a monotonous increase and a monotonous decrease with increasing temperature, respectively. For structure "e" at this pressure value, we observe discontinuous changes both in $U^\star$ and η at $T^\star \simeq 0.05$ indicating a structural change that occurs with increasing temperature. The main feature of this transition is a reorientation of the particles, so that one well-aligned patch-patch bond is replaced by two weaker bonds with less optimal alignment. As mentioned above, the high temperature version of structure "e" (i.e., the one with two weaker bonds) has a region of stability in the phase diagram. We note that when cooling this structure down again, we do not recover structure "e" (see the dotted blue lines in Fig 4). Instead at low temperature we obtain a structure with slightly lower packing fraction but much higher energy. We have not studied this issue further, but it is possible that a different behaviour is observed by changing the speed of quenching.

3.2. Structural variations along isotherms

In Figure 5 we have depicted $U^\star$ and η (both obtained via simulations) along the isotherm $T^\star = 0.10$ over a relatively large pressure interval, namely $P^\star \in [2, 10]$. Values for the two quantities are depicted for structures labeled "b", "d", "e", "f", "g", and "h" over the respective ranges of stability; we note that mechanical stability (i.e., a positive compressibility) is guaranteed as long as η increases monotonically with increasing pressure. The corresponding values for the lattice "a" coincide with the values of "b" within line-thickness and lattice "c" is stable only for $T^\star \lesssim 0.006$ (see discussion above). As can be seen from the phase diagram presented in [8], at this temperature the system forms at low pressure values structure "b", which transforms at $P^\star \simeq 4.06$ into structure "e" and eventually at $P^\star \simeq 6.27$ into structure "f".

Finally, Figure 6 shows the enthalpy $H^\star$ for $T^\star = 0$ and the chemical potential $\mu^\star$ along two different isotherms (i.e., $T^\star = 0.05$ and $T^\star = 0.10$) over the narrow pressure ranges where a phase transition between two competing structures takes place. The top panel shows for $T^\star = 0$ the enthalpy values in a $P^\star$-range where the system transforms – with increasing pressure – from a double diamond ("a") to a double diamond/bcc broken ("c") lattice which eventually transforms into a fcc-like structure ("f"). For clarity the respective curves of the other structures are not shown since they differ only by small amounts of the respective values of the three energetically most favourable lattices. The central panel of Figure 6 focuses on the transition region from structure "b" to lattice "f" along the isotherm $T^\star = 0.05$. Again only minute differences in the thermodynamic properties (here: the chemical potential) decide which is the energetically most favourable ordered structure. Finally the bottom panel of this Figure shows the chemical potential $\mu^\star$ along the isotherm $T^\star = 0.10$, focusing on the transition region between structures "b" and "e". Again, the curves for the other competing structures, characterized by (slightly) higher chemical potential values are not shown for clarity. Table 1 shows data for the chemical potential for the phase transition between structures "e" and "f" at $T^\star = 0.10$, where the differences in the respective $\mu^\star$-values of the competing structures are too small to be depicted in a figure. This indicates the strong competition between the candidate structures.

4. Conclusions

We have investigated the ordered equilibrium structures of patchy particles with a regular tetrahedral patch decoration. To this end we have identified at *vanishing* temperature with a reliable and efficient optimization tool the ordered structures that correspond in an NPT ensemble to the lowest-lying local enthalpy minima. With these candidate structures at hand, we have calculated with a suitably adapted Monte Carlo simulation technique, the thermodynamic properties of these lattices at *finite* temperature via thermodynamic integration. With this combination of two complementary approaches we compensate for the respective limitations of the two

methods: the reliability of the optimization tool avoids – by providing a comprehensive set of candidate structures for the evaluation of the phase diagram – that possible equilibrium structures are simply forgotten; the computer simulations allow an accurate evaluation of the thermodynamic properties of the suggested candidate structures at any finite temperature and any pressure value.

Based on the knowledge of the entire (pressure vs. temperature) phase diagram [8] we have studied the thermodynamic properties of these candidate structures along selected isobars and isotherms in detail. To this end we have split up the respective enthalpy values into their relevant contributions, namely energy (i.e., the lattice sum) and volume (i.e., the packing fraction). From these detailed investigations it becomes obvious that the selection of the energetically most favourable lattice structure at a given state point is the result of a strong competition between the two above mentioned contributions to the thermodynamic potential. Already at vanishing temperature, unsaturated bonds of a given ordered structure (leading to a higher value of the lattice sum) may be compensated by a dense packing, leading to a lower enthalpy value, compared to a lattice with better bond saturation but a smaller packing fraction. As temperature is included, entropy enters the competition between these two contributions and the situation becomes even more intricate.

In particular we learn that – even though an ordered structure might correspond only to a local minimum in enthalpy at vanishing temperature – this structure can turn out to be the energetically most favourable lattice in some pressure- and temperature-range. Thus, it is necessary to consider such local enthalpy minima as possible candidate structures when evaluating the phase diagram of patchy particles.

Acknowledgments

Financial support by the Austrian Science Foundation (FWF) under project Nos. W004, M1170-N16 and P23910-N16 is gratefully acknowledged. E.G.N. gratefully acknowledges support from Grants Nos. FIS2010-15502 from the Direccion General de Investigacion and S2009/ESP-1691 (program MODELICO) form the Comunidad Autonoma de Madrid.

References

[1] Pawar A B and Kretzschmar I 2010 *Macromol. Rapid. Commun.* **31** 150
[2] Bianchi E, Blaak R and Likos C N 2011 *Phys. Chem. Chem. Phys.* **13** 6397
[3] Zhang Z L, Keys A S, Chen T and Glotzer S C 2005 *Langmuir* **21** 11547
[4] Wilber A W, Doye J P K, Louis A A, Noya E G, Miller M A and Wong P 2007 *J. Chem. Phys.* **127** 085106
[5] Noya E G, Vega C, Doye J P K and Louis A A 2010 *J. Chem. Phys.* **132** 234511
[6] Romano F and Sciortino F 2011 *Nature Mater.* **10** 171
[7] Romano F, Sanz E and Sciortino F 2011 *J. Chem. Phys.* **134** 174502
[8] Doppelbauer G, Noya E G, Bianchi E and Kahl G 2011 *submitted* arxiv:1201.3259v2 [cond-mat.soft]
[9] Doppelbauer G, Bianchi E and Kahl G 2010 *J. Phys.: Condens. Matter* **22** 104105
[10] Frenkel D and Ladd A J C 1984 *J. Chem. Phys.* **81** 3188
[11] Vega C and Noya E G 2007 *J. Chem. Phys.* **127** 154113
[12] Romano F, Sanz E and Sciortino F 2010 *J. Chem. Phys.* **132** 184501
[13] Doye J P K, Louis A A, Lin I C, Allen L R, Noya E G, Wilber A W, Kok H C and Lyus R 2007 *Phys. Chem. Chem. Phys.* **9** 2197
[14] Noya E G, Vega C, Doye J P K and Louis A A 2007 *J. Chem. Phys.* **127** 054501
[15] Williamson A J, Wilber A W, Doye J P K and Louis A A 2011 *Soft Matter* **7** 3423
[16] van der Linden M, Doye J P K and Louis A A 2012 *J. Chem. Phys.* **136** 054904
[17] Antlanger M, Doppelbauer G and Kahl G 2011 *J. Phys.: Condens. Matter* **23** 404206
[18] Zhu C, Byrd R H, Nocedal J 1997 *ACM Trans. Math. Software* **23** 550
[19] Gottwald D, Kahl G and Likos C N 2005 *J. Chem. Phys.* **122** 204503
[20] Pauschenwein G J and Kahl G 2008 *J. Chem. Phys.* **129** 174107
[21] Kahn M, Weis J J and Kahl G 2010 *J. Chem. Phys.* **133** 224504
[22] Maldovan M and Thomas E L 2004 *Nature Mater.* **3** 593
[23] For double diamond/bcc-like structures, particles belonging to different non-interacting diamond sublattices appear in different colours. For structures consisting of hexagonal layers, particles located in different layers are coloured in an alternating pattern. For fcc-like structures, the particles located at the vertices of the cube and the particles at the centers of the faces of the cube are coloured red and yellow, respectively.

$P^\star$	$\mu^\star$ (fcc-like 1 ⓔ)	$\mu^\star$ (fcc-like 2 ⓕ)
6.00	51.29	51.37
6.10	52.11	52.14
6.20	52.90	52.92
6.30	53.70	53.69
6.40	54.49	54.47
6.50	55.29	55.23
6.60	56.08	55.98

Table 1. Addendum to Figure 6: Reduced chemical potential $\mu^\star$ at $T^\star = 0.10$ of the structures "e" and "f" for $P^\star$-values in the vicinity of the phase transition between these structures. (The values are too close for a clear visual representation in a graph)

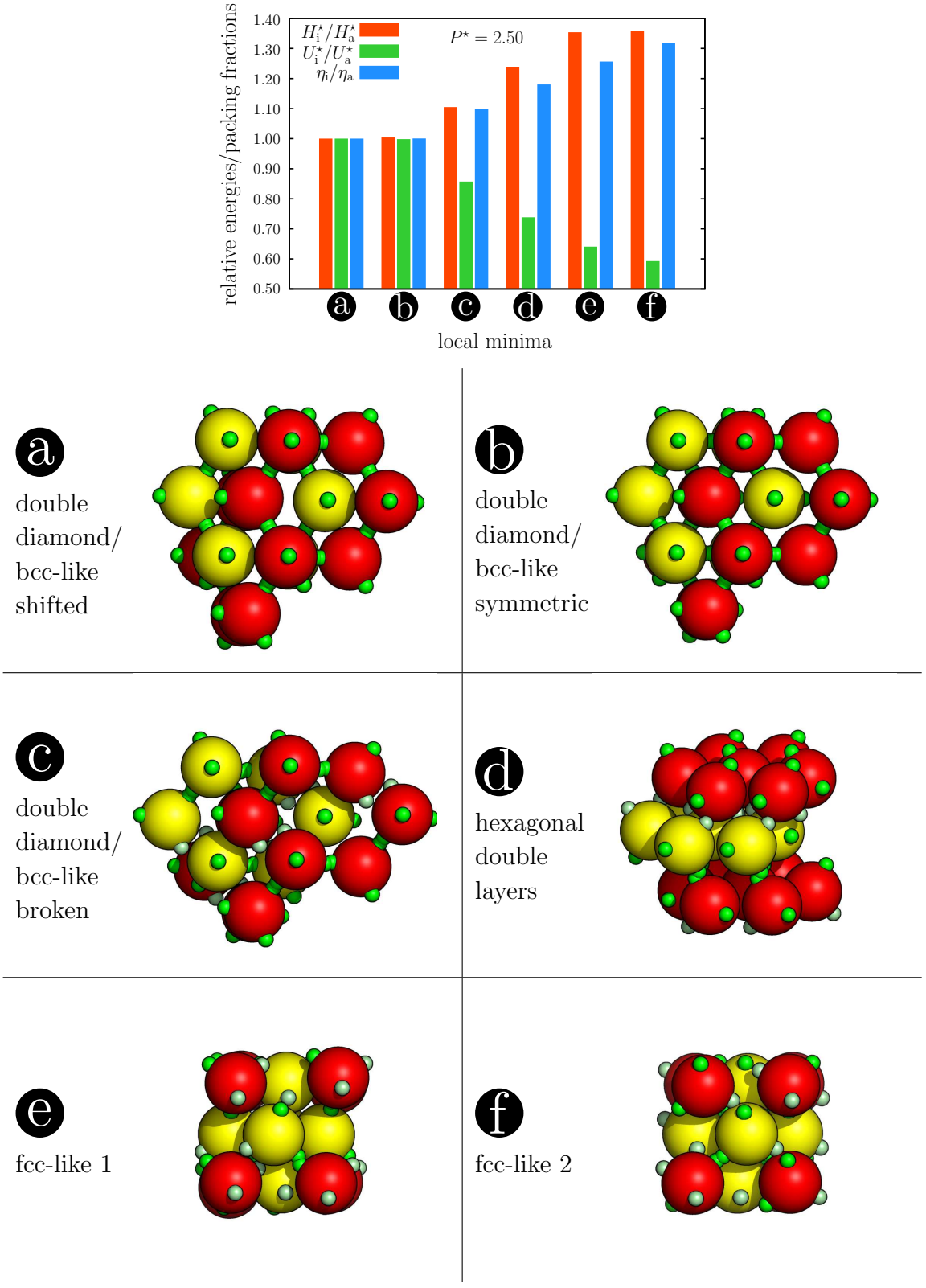

Figure 1. (Colour online) Top panel: enthalpies $H_i^\star$, binding energies (i.e., lattice sums) $U_i^\star$, and packing fractions η_i of the six lowest, structurally different local enthalpy minima identified by the evolutionary algorithm for $P^\star = 2.50$ with i = "a" to "f". Values are given in units of the respective values of the energetically most favourable lattice ("a"). Other panels: visual representations of these structures as labeled. Particles are coloured red and yellow as a guide to the eye [23]. Fully bonded patches are coloured bright green, weakly- or non-bonded patches are shown in pale green. Structures "a", "b", "c", "e", and "f" are thermodynamically stable in certain regions of the $(P^\star, T^\star)$-phase diagram (cf. [8]).

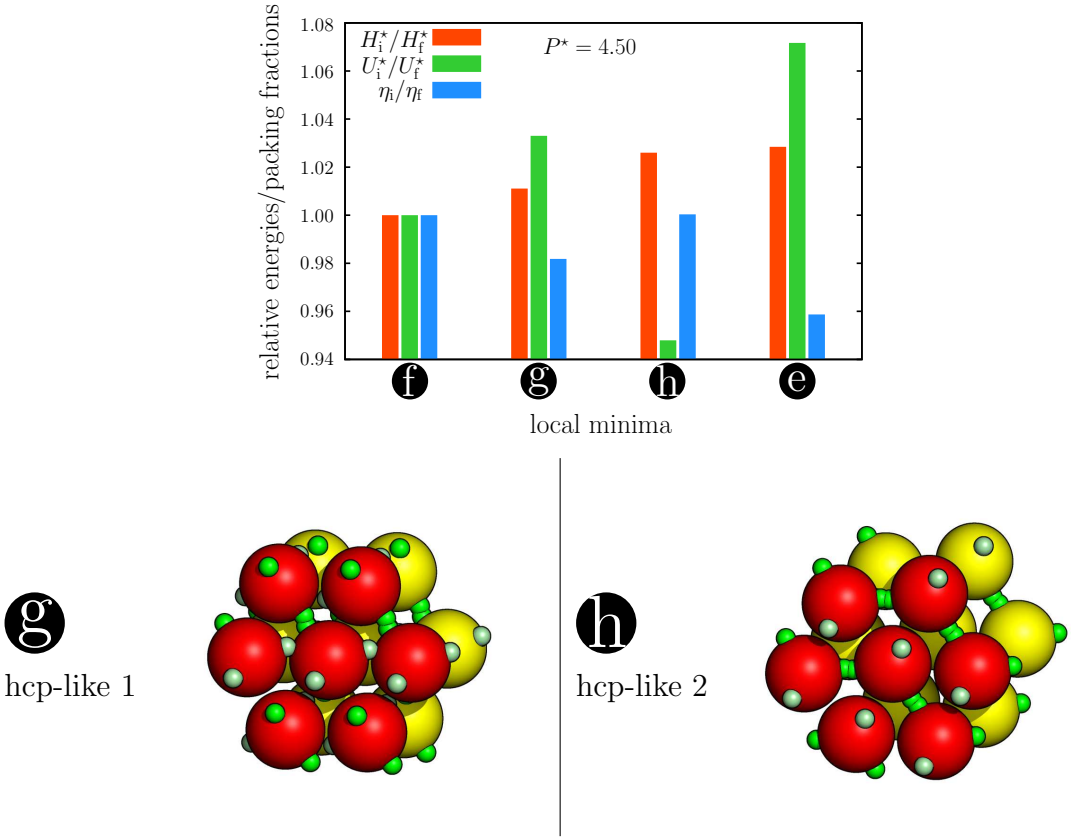

Figure 2. (Colour online) Top panel: enthalpies $H_i^\star$, binding energies (i.e., lattice sums) $U_i^\star$, and packing fractions η_i of the four lowest, structurally different local enthalpy minima identified by the evolutionary algorithm for $P^\star = 4.50$ with i = "e" to "h". Values are given in units of the respective values of the energetically most favourable lattice ("f"). Other panels: visual representations of structures "g" and "h"; the other two lattices are displayed in Figure 1. Particles are coloured red and yellow as a guide to the eye [23]. Fully bonded patches are coloured bright green, weakly- or non-bonded patches are shown in pale green. Structures "e" and "f" are thermodynamically stable in certain regions of the $(P^\star, T^\star)$-phase diagram (cf. [8]).

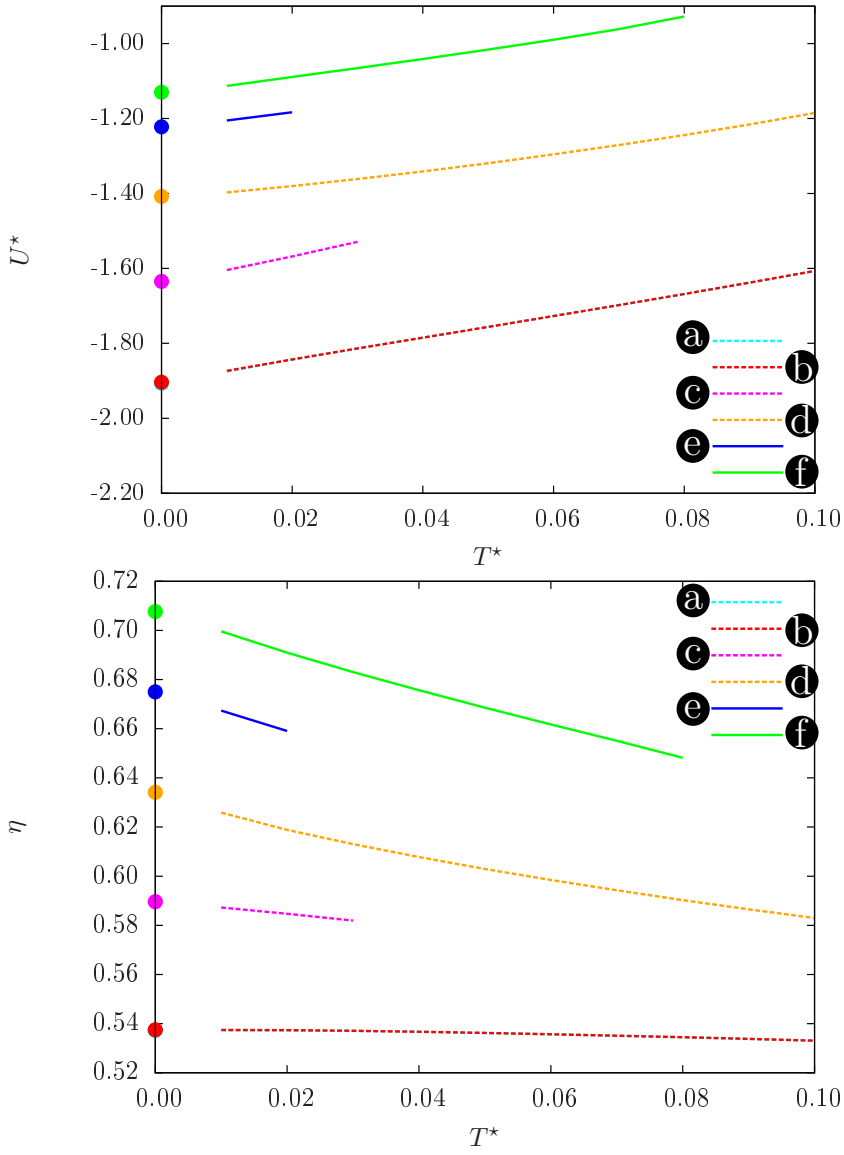

Figure 3. (Colour online) Reduced binding energy (i.e., lattice sum) $U^\star$ (top panel) and packing fraction η (bottom panel) of six different competing crystal structures as functions of temperature $T^\star$, obtained from MC simulations. These lattices have been identified as low-lying local enthalpy minima along the isobar $P^\star = 2.50$. The lines for the double diamond/bcc shifted lattice ("a") and the double diamond/bcc symmetric structure ("b") coincide within line-thickness. Data are shown only over the temperature ranges where the respective structures are mechanically stable. Dots on the vertical axes (i.e., $T^\star = 0$) represent results for $U^\star$ and η obtained from the evolutionary algorithm.

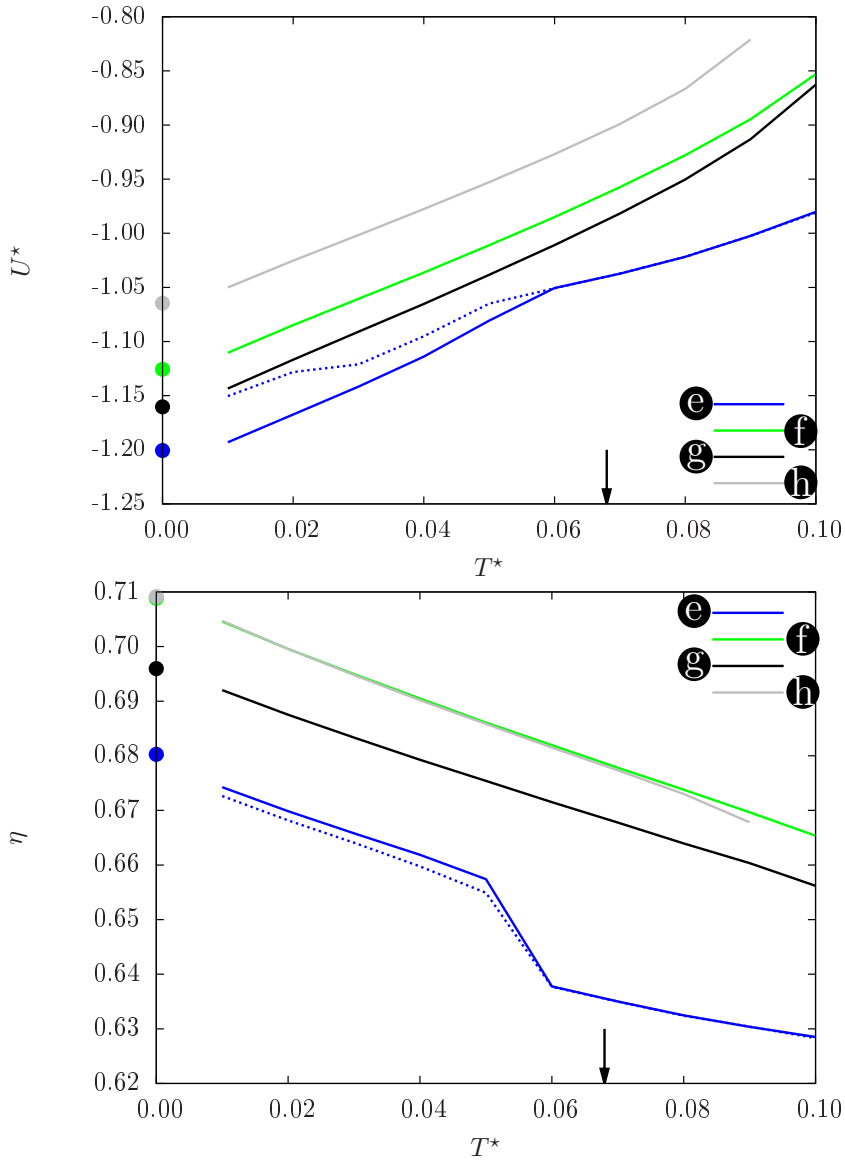

Figure 4. (Colour online) Reduced binding energy (i.e., lattice sum) $U^\star$ (top panel) and packing fraction η (bottom panel) of four different competing crystal structures as functions of temperature $T^\star$, obtained from MC simulations. These lattices have been identified as low-lying local enthalpy minima along the isobar $P^\star = 4.50$. Data are shown only over the temperature ranges where the respective structures are mechanically stable. Dots on the vertical axes (i.e., $T^\star = 0$) represent results for $U^\star$ and η obtained from the evolutionary algorithm. The vertical arrow indicates the temperature values where a structural phase transition takes place (i.e., between structures "e" and "f" at $T^\star = 0.068$). For a discussion of the dotted blue lines, we refer to the main text.

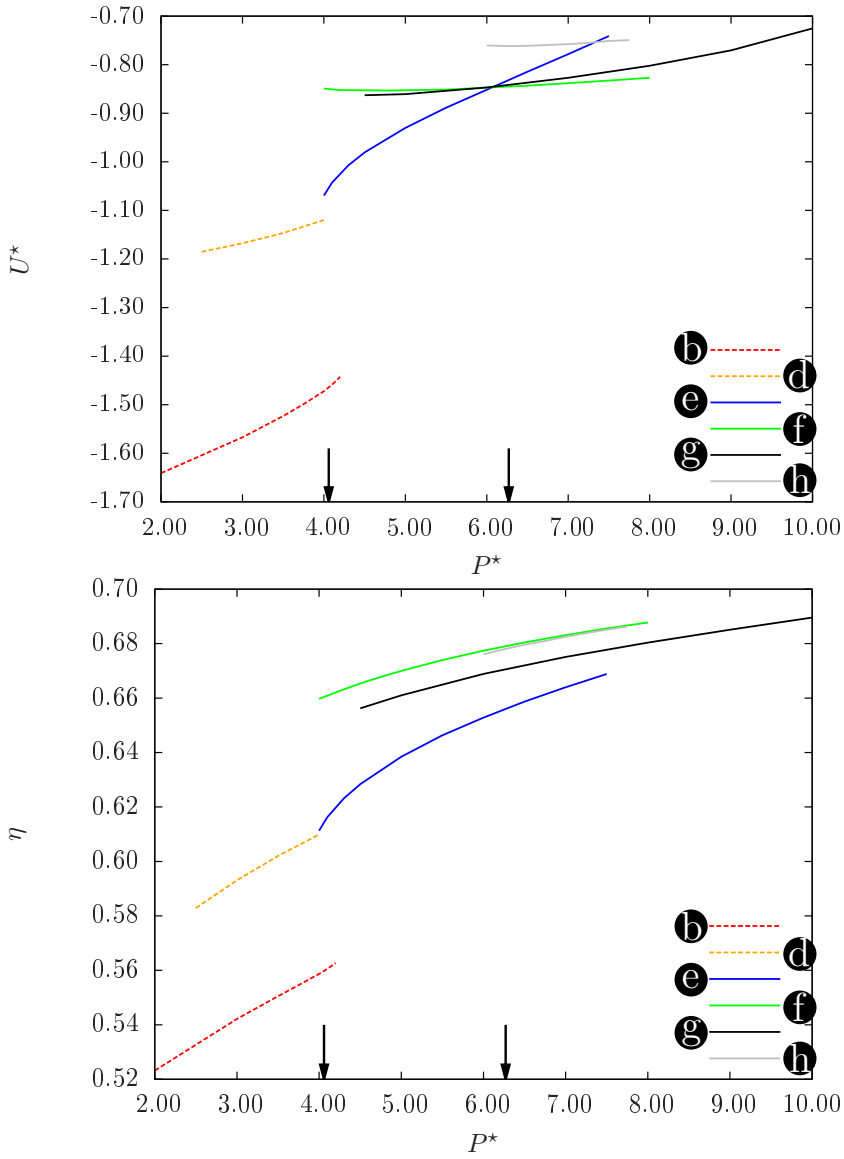

Figure 5. (Color online) Reduced binding energy (i.e., lattice sum) $U^\star$ (top panel) and packing fraction η (bottom panel) as functions of $P^\star$ along the isotherm $T^\star = 0.10$. Results have been evaluated for the different crystal structures via MC simulations. The data are plotted only over the ranges of mechanical stability of the respective structures. The vertical arrows indicate those pressure values where structural phase transitions take place (i.e., between structures "b" and "e" at $P^\star = 4.06$ and between structures "e" and "f" at $P^\star = 6.27$).

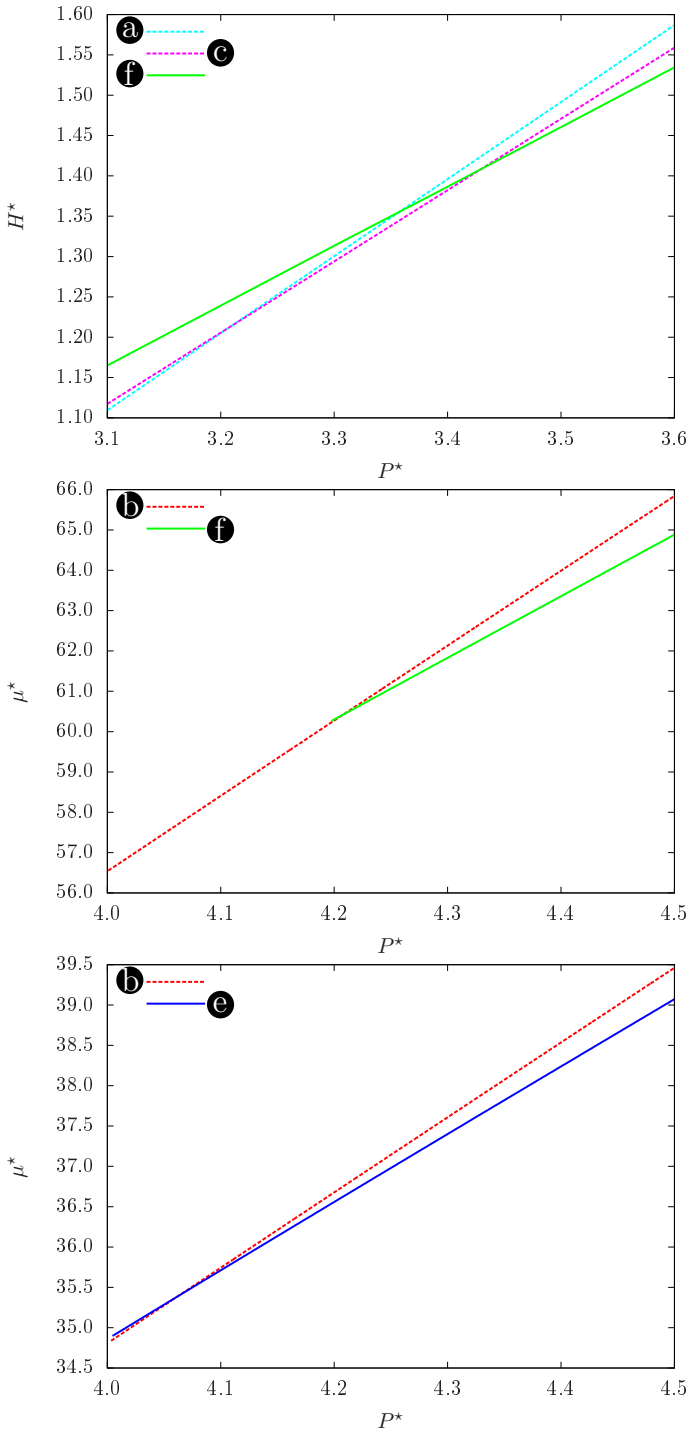

Figure 6. (Colour online) Top panel: reduced enthalpy $H^\star$ at vanishing $T^\star$ as a function of $P^\star$ in the vicinity of the phase transition between the ordered structures "a", "c", and "f" – cf. phase diagram shown in [8]. Center panel: reduced chemical potential $\mu^\star$ as a function of $P^\star$ along the isotherm $T^\star = 0.05$ in the vicinity of the phase transition between the ordered structures "b" and "f". Bottom panel: reduced chemical potential $\mu^\star$ as a function of $P^\star$ along the isotherm $T^\star = 0.10$ in the vicinity of the phase transition between the ordered structures "b" and "e". The respective values in the vicinity of the phase transition between structures "e" and "f" are summarized in Table 1.